Late-acting self-incompatible system, preferential allogamy and delayed selfing in the heterostylous invasive populations of *Ludwigia grandiflora* subsp. *hexapetala*

Luis O. PORTILLO LEMUS[1], Marilyne HARANG[1], Michel BOZEC[1], Jacques HAURY[1], Solenn STOECKEL[2], Dominique BARLOY[1]

Short title: Mixed mating system in a European invasive Ludwigia

[1] ESE, Ecology and Ecosystem Health, Institut Agro, INRAE, 35042, Rennes, France

[2] IGEPP, INRAE, Institut Agro, Univ Rennes, 35653, Le Rheu, France

Corresponding author: dominique.barloy@agrocampus-ouest.fr

Orcid number:

Luis O. PORTILLO LEMUS: 0000-0003-2123-4714

Jacques HAURY: 0000-0002-8628-8265

Solenn STOECKEL: 0000-0001-6064-5941

Dominique BARLOY: 0000-0001-5810-4871

Abstract

Mating system influences local population genetic structure, effective size, offspring fitness and functional variation. Determining the respective importance of self- and cross-fertilization in hermaphroditic flowering plants is thus important to understand their ecology and evolution. The worldwide invasive species, *Ludwigia grandiflora* subsp. *hexapetala* (*Lgh*) presents two floral morphs: one self-compatible short-styled morph (S-morph) and one self-

incompatible long-styled morph (L-morph). Most invasive populations worldwide are only composed of self-incompatible L-morphs, which questions the importance of sexual reproduction during the invasion. In this study, we identified the mating systems of western European experimental and natural populations of *Lgh* by comparing structural characteristics of pollen and style, by studying self- and cross-pollen tube elongations and the viability of the resulting seeds and seedlings in both morphs. Our results showed no differences in pollen shape and stigma surfaces among and between the two floral morphs. In the self-incompatible L-morph flowers, self-pollen tubes were stopped tardily, in the ovarian area, and were unable to fertilize the ovules. This first formal identification of a late-acting, prezygotic self-incompatible system in *Ludwigia* genus questions on the distribution of this mating system in the Myrtales order. In the self-compatible S-morph flowers, rarer in worldwide invasive populations, self-pollen always succeeded to self-fertilize the ovules that nearly all developed into viable seedlings. However, cross-pollen tubes always elongated faster than self-pollen tubes. S-morph individuals may thus advantage preferential allogamy over selfing when cross-pollen is available despite its self-compatibility. As expected in late-acting self-incompatible systems, L-morph flowers authorised 0.2‰ of selfed seeds during the uppermost flowering season, that increased to 1‰ at the end of the flowering season. Such delayed selfing resulting in a significant quantity of viable floating seeds may contribute to the local regeneration, seed bank and propagation of the L-morph, which may explain its invasion success worldwide. Management plans of *Lgh* would gain to consider the mixed mating system we identified.

Keywords: Delayed selfing, Mating system, Onagraceae, Pollen tube elongation, Reproductive assurance, Self-fertilization, Water primrose

Introduction

Around 50% of angiosperm species develop a variety of self-incompatible mechanisms (SI) that favour allogamy by avoiding self-fertilisation and promoting outcrossing (Igic et al. 2008; Fujii et al. 2016). Characterizing the type of SI by identifying the site of the pollen-pistil recognition within species is essential to categorize and assess the prevalence of SI systems across Angiosperms and beyond, and understand their phylogeny and evolution (Charlesworth et al. 2005; Igic et al. 2008; Santos-Gally et al. 2013; Gibbs 2014a; Fujii et al. 2016; Grossenbacher et al. 2017; Barrett 2019). Moreover, identifying the type of SI mechanism developed by specific species and populations helps understanding plant ecology and evolution, including how their mating systems may contribute to their adaptation in a context of global changes (Charlesworth et al. 2005; Takayama and Isogai 2005; Busch and Schoen 2008; Ferrer and Good 2012; Grossenbacher et al. 2017). Mating systems are indeed the main factor influencing the evolution of genetic diversity in populations and species with potential consequences for adaptation and peripatric speciation (Duminil et al. 2007; Ellegren and Galtier 2016).

We currently consider three major mechanisms of self-incompatibility in flowering plants, homomorphic gametophytic, homomorphic sporophytic and heteromorphic sporophytic, that differ in the site of the rejection of incompatible pollen tubes (Gibbs and Bryan 1986; Dickinson et al. 1992; Hinata et al. 1993; Barrett and Cruzan 1994b; Kao and McCubbin 1996; de Nettancourt 1997). Homomorphic SI systems imply that flowers with different SI types present the same flower shape and structure. By contrast, heteromorphic self-incompatibility (HetSI) associates different SI systems with different flower structure such as heterostyly (Darwin 1877; Barrett and Cruzan 1994a; Igic et al. 2004; Barrett 2019). Heterostyly defines the occurrence in a species of two or three floral morphs (di- and tristyly) that exhibit reciprocal herkogamy (spatial distancing of the anthers and stigma in the 3D

architecture of a flower, Barranco et al. 2019), sometimes associated with additional features such as differences in pollen sizes and shapes, and different lengths of stigmatic papillae (Barrett and Shore 2008). Commonly, species with style polymorphism have a sporophytic heteromorphic (*i.e.* di- or tri-allelic) incompatibility system that prevents self-fertilization and crosses between individuals of the same floral morph (Barrett 2019).

In most studied species developing these three SI systems, pollen-tube growth is stopped from the stigma or in the style as a result of a rapid response to the pollen–pistil interaction. However, some species present a delayed reaction of self-pollen rejection, named ovarian or late-acting self-incompatibility (LSI) because occurring lately in the ovarian area (Seavey and Bawa 1986; Gibbs and Bianchi 1993; Sage et al. 1994; Gibbs 2014a). It often coincides with a residual permeability of their SI systems resulting in a steady low level of selfing despite an effective late-acting SI (Seavey and Bawa 1986; Gibbs 2014a). It concerns both homomorphic and heterostylous species (Gibbs 2014a; Simon-Porcar et al. 2015). For example, the homomorphic LSI Theaceae species *Camelia oleifera* and *Camelia sinensis,* allow 10% and ~2% of self-fertilization resulting in viable seeds, respectively (Chen et al. 2012; Liao et al. 2014). In the ovarian LSI heterostylous *Narcissus spp.* from the Amarilidacea, from 4 to 30% of their seed-sets result from self-fertilization (Barrett et al. 2004; Medrano et al. 2012; Simon-Porcar et al. 2015). Within literally pre-zygotic LSI, Gibbs (2014) proposes to distinguish LSI mechanisms stopping pollen tubes before ovaries (as found in *Melaleuca spp*. and *Thryptomene calycina,* Barlow and Forrester 1984; Beardsell et al. 1993) from those stopping self-pollen tubes while penetrating the ovules (as found in *Acacia retinodes,* Kenrick et al. 1986).

In the Ludwigia genus (Onagraceae), 8 of 82 species have been reported as "self-incompatible", although the nature of their SI were not formally studied and established (Raven 1979). Water primrose, *Ludwigia grandiflora* subsp. *hexapetala* (Hook. & Arn.) Nesom and Kartesz (2000), (hereafter *Lgh*), is one of the most invasive aquatic plants in the world

(Thouvenot et al. 2013). Tackling how this species reproduces is crucial for understanding how to slow its expansion and alleviate its impacts in the invaded aquatic environments (EPPO, 2011). Yet, we still don't know how sexual reproduction contributes to the invasiveness of the species in the newly-colonized areas (Dandelot 2004; Ruaux 2008; Thouvenot et al. 2013). This species presents two types of heterostylous flowers in European invasive populations: a short-styled morph (S-morph) that is self- and intra-morph compatible (crosses produce viable seeds), and a long-styled morph (L-morph) that is self- and intra-morph incompatible (crosses do not produce seeds, Portillo-Lemus et al. 2021). In both floral morphs, inter-morph crosses always produce viable seeds. The two floral morphs of *Lgh* develop bowl-shaped non-tubular flowers with two whorls of stamens of different heights. In the L-morph flowers, stamens of the second whorl (inner whorl) are longer than these of the first whorl (outer whorl). These two characteristics contrast with typical heteromorphic SI species that most frequently present tubular flowers and only one whorl of stamens (Barrett and Shore 2008; Cohen 2010; Barrett 2019). Interestingly, floral morphs are mostly found in allopatric monomorphic populations (*i.e.,* exclusively S-morph or exclusively L-morph populations) in Western Europe and other invasive worldwide populations (Hieda et al. 2020; Portillo-Lemus et al. 2021). Surprisingly, around 75% of the invasive populations worldwide are exclusively composed of self-incompatible L-morph individuals, tackling the paradigm that successful invasive species may be mostly composed of individuals able to reproduce using self-fertilization (Baker 1955; Cheptou 2012; Razanajatovo et al. 2016). Recently, some isolated monomorphic L-morph self-incompatible populations were however found to produce seeds (Portillo-Lemus et al. 2021). These puzzling observations question the type of SI reaction involved in the self-incompatible L-morph and its level of permeability to self -fertilization. More broadly, they question the type of mating systems developed in these invasive populations and the respective importance of allogamy and selfing during invasion (Hieda et al. 2020; Portillo-Lemus et al. 2021).

In this study, we thus aimed at better characterizing the mating system of the two floral morphs in Western European populations of *Lgh* by tracking the fates of self- and inter-morph pollen tubes in both floral morphs. First, we searched for structural evidences through analysis of the morphologies of pollen grains and stigma surfaces of the two floral morphs that may be characteristic of homomorphic and heteromorphic sporophytic self-incompatibilities. Second, to better categorize the type of the SI developed by this species, we aimed at identifying the site of the self-pollen rejection in the self-incompatible L-morph individuals. To achieve this goal, we followed the germination and the progression of the self- and inter-morph-pollen tubes on histological sections, prepared at different times after pollination. Third, to quantify the permeability of this self-incompatible system, we counted the number of viable seeds and seedlings obtained from self-fertilization in controlled conditions and in natural monomorphic L-morph populations. Fourth, to test if the S-morph individuals truly reproduced using selfing, as expected in this self-compatible morph, we followed the progression of the self- and inter-morph-pollen tubes, as described for the morph-L, and studied the viability of obtained seeds and seedlings. Finally, we compared the results we obtained with other species, especially from the Myrtales order to discuss on the importance of our results for our phylogenetic comprehension of SI distribution in these families.

Materials and Methods

Plant material and sampling populations

To better characterize the mating system of the two floral morphs previously reported in *Lgh*, (Portillo-Lemus et al. 2021), we focused our study on individuals sampled from five monomorphic fruitful populations only composed of S-morph individuals and from five

monomorphic fruitless populations only composed of L-morph individuals, growing along the Loire valley in France (Table S1 for GPS location). We sampled 10 stems per population that were transplanted into a common greenhouse (location: Agrocampus Ouest, Rennes, France. 48°06'47.7"N 1°42'30.2"W). All individuals sampled from one population were growth together in an 80L container. The 10 containers were watered every 15 days with a commercial nutrient solution (6% nitrogen, 6% phosphorus and 6% potassium) during growth and flowering periods to avoid nutritional deficiencies.

Histological preparations

To observe pollen and stigmatic papillae morphology, to follow pollen tube growth and to achieve histological sections of ovaries for studying embryo development, we fixed flowers in FAA 1: 2: 20 (formalin: acetic acid: ethanol V/V). Pollen germination, pollen tube growth and ovule penetration were observed using the aniline blue fluorescence method (Martin 1959). The fixed samples were washed several times with distilled water and each flower was placed in 1mL of staining solution (0.1% w/v aniline blue, 1% v/v tween-20$^{(R)}$, 0.2 M K_2PO^4, 0.1 M NaOH) for 1 hour at 95°C. After squashing the pistils between the slide and coverslip, observations were made under ultraviolet light (335-364 nm) with a microscope Leica DM4000 B$^{©}$, and a camera 190HD. To observe embryo development, fixed ovaries were dehydrated, embedded in paraffin, sectioned at 15 µm with a microtome, and mounted on glass slides (Sakai, 1973). Sections were placed in 0.05% toluidine blue O in distilled water for 2–30 min, rinsed once in water for 1 min, and air-dried. Paraffin was removed using two xylene baths and the cover slip was mounted with resin. Histological preparations were realized by Nublat Laboratory (https://www.laboratoire-nublat.com/118botanique.html).

Pollen and stigmatic papillae morphologies

To assess if heterostylous flowers of *Lgh* showed difference in pollen shapes and sizes in association with floral morphs, we studied the shape of 500 pollen grains per floral morph. For each morph, we sampled 25 flowers in the 5 corresponding populations. For each of these flowers, we measured 20 pollen grains from a mix of the stamen verticels, resulting into a total of 1000 pollen grain measures for both morphs. We measured their diameter under an optical microscope. To assess if heterostylous flowers of *Lgh* showed difference in stigmatic papillae structure as expected in classical heteromorphic SI species, we also noted the long or short shape of stigmatic papillae in 30 histological stylar sections for each of the two floral morphs (Dulberger 1992).

Pollen tube growth, ovule fertilisation and embryo-sac development

To identify the site of the self-pollen rejection in the L-morph pistil and to characterize the type of mating preferentially achieved in the two floral morphs, we performed hand-controlled pollinations to track and compare the self- and inter-morph pollen tube growth in both floral morphs. As experimental pollinations in *Lgh* have previously shown that self- and intra-morph pollinations in L-morph flowers lead to a similar incompatible reaction (Portillo Lemus et al 2021), we focused our experiments here on a comparison between self-pollinations (pollen grains from the same flowers) and reciprocal inter-morph pollinations. To perform controlled self-pollinations, we enclosed early flower buds in cellophane bags to protect them from external pollen. To effect self-pollination, we dissected mature anthers using tweezers to place pollen directly on its own receptive stigma and re-enclosed the flowers in cellophane bags. For reciprocal inter-morph pollination, to simulate free random crosses, we selected five pollen-donor flowers from short-style or long-style flowers to create a pollen mix. Flowers to receive

pollen were emasculated before anthesis and then pollinated with this mix of pollen. After pollination, the pollinated flowers were once again enclosed in cellophane bags in order to protect them from any contaminant pollen.

To study self- and inter-morph pollen tube growth in both floral morphs, we made 150 self-pollinations per morph and 300 reciprocal disassortative pollinations between S-morph and L-morph. At 2, 3, 7, 16, 24 hours after the hand-controlled pollination, we randomly sampled and fixed 30 flowers per morph and pollination type. For each flower, pollen tube growth and ovule fertilisation were observed using aniline blue fluorescence method with squashed pistils. We measured the growth of the pollen tubes, *i.e.*, the distance between the stigma and the tip of pollen tube (d, µm) at 2, 3, 7, 16, 24 hours (*t*) after the hand-controlled pollinations. From these measures, we calculated the speed of pollen tube (speed) between two measures in micrometres per hour (µm/h) as $speed = \frac{d_{t_2} - d_{t_1}}{t_2 - t_1}$ and the acceleration of pollen tube growth in micrometres per hour square (µm/h²) as $acceleration = \frac{speed_{t_2} - speed_{t_1}}{t_2 - t_1}$.

To evaluate the viability of fertilisation and study the embryo-sac development, we analysed a total of 2520 ovary sections corresponding to 14 sections of five flowers per floral morph and cross type, over nine-time steps (1, 2, 3, 4, 5, 6, 7, 15, 21 days after pollination (*dap*).

Fruit and seed set production

To assess the incidence of self-fertilisation in the self-incompatible L-morph individuals, 1600 self-pollinations were carried out from July to August (summer), and from September to October (fall), respectively. Self-pollinated L-morph flowers were randomly selected within groups of individuals growing in the greenhouse. As a control, we made 30 self-pollinations

with self-compatible S-morph flowers, 30 L x S and 30 S x L-morph pollinations during summer and repeated this sequence during the fall.

We also assessed the rate of self-fertilisation in self-incompatible L-morph from *in situ* populations at the beginning of October. We collected the fruits of five S-morph and five L-morph *in situ* populations to evaluate the fruit and seed sets. To quantify the fruit-set *in situ*, we counted fruits produced in five quadrats of 1 m^2, 10 m away on a linear transect. As S-morph populations showed a massive fruit production, we estimated the seed-set production per m^2 as the mean number of seeds produced by 25 fruits randomly picked in the quadrats (5 fruits per quadrat). As the L-morph *in-situ* populations produced few fruits, we collected and counted all the seeds produced in all the fruits found in quadrats. We sowed all the *in-situ* produced seeds in the greenhouse to calculate the germination rate as the number of seedlings over the number of sowed seeds.

Statistical analysis

To examine possible differences in pollen tube elongations at each time step (time=[2, 3, 7, 16, 24 hours]), and the changes in speed and acceleration of elongations along time in the styles of the two floral morphs considering the four possible types of crosses (cross_types=[S-morph self-pollination; S-morph x L-morph; L-morph self-pollination; L-morph x S-morph]), we used ANOVA (type = III) tests. For each time step, we computed three ANOVA models: pollen_tube_length~cross_types, speed~cross_types*time and acceleration~cross_types*time. For each test, we verified the homoscedasticity of distributions between groups and the normality of residuals using Shapiro–Wilk's tests. When ANOVAs were significant, we applied Tukey’s honestly significant difference (HSD) posthoc comparisons of the means to identify which groups and parameters caused those significant differences. All analyses were performed

using the stats package in R 4.0.4 software (R Development Core Team, 2014). All results were summarised in the supplementary information table S2.

Results

Pollen and stigmatic papillae morphologies

Pollen grains were all released in triporate monads and connected to the anthers by viscin threads (Fig.1; a3). In both floral morphs and in all the studied populations, pollen grains were all smooth and had the same sizes ranging from 60 to 95 µm whatever their floral morphs (ANOVA, p-value=0.228, Fig. 1 b3, c3). The styles of both floral morphs had capitate stigmas, which were all wet during anthesis and had stigmatic papillae which were submerged by mucilage (Fig. 1; a1, b1). In both floral morphs, all the 60 longitudinal sections of the stigma receptive surface (30 per morph) showed the same morphology of elongated unicellular papillae (Fig. 1; a2, b2). The only difference we found between styles of floral morphs concerned their lengths: styles of S-morph flowers were significantly wider (2.27mm ± 0.19) and shorter (8.04 mm ± 0.19) than those of L-morph flowers (width: 1.53 mm±0.09; length: M=8.97±0.25; p-value=$<10^{-15}$, Fig.1; c1, c2), resulting in a difference of around 1mm between long- and short-style lengths.

Pollen tube growth and fertilisation

All pollen grains germinated, elongated down the style (Fig. 2a-c), and reached the ovules 24 hours after pollen deposition on stigmas (Fig. 2d-e), in self and inter-morph crosses and whatever the pollen origin. In the self-pollinated L-morph flowers, only six ovules of 300 studied (2 %) were penetrated by a pollen tube with pollen tube tips located in the area of the

embryo sac (Fig. 2f). Figure 2f shows an ovule surrounded by several pollen tubes, but it is unclear whether any of them have penetrated the micropyle. The other 294 unpenetrated ovules showed tips of pollen tubes with a small bulge, stopped between the ovarian tissues and the beginning of the first cell layers of the ovule integuments and we found no traces of pollen tubes in the area of the embryo sac (Fig. 2d, e). All the 300 L-morph ovules that were cross-pollinated with S-morph pollen were penetrated by pollen tubes 24 hours after pollination. All S-morph ovules were penetrated by one pollen tube 24 hours after self and inter-morph pollinations (Fig. 2g).

Kinetic elongation of pollen tube

In the styles of both floral morphs, until reaching the ovules, inter-morph pollen tubes outdistanced self-pollen tubes (HDS-test, p-value=$<10^{-15}$; Mean and SD values reported in Table S2; Fig. 3). Significant advances of inter-morph pollen tubes were observed from two hours after pollinations. (Fig. S1a). Speed of elongations of pollen tubes in both morphs quickly increased in the first two hours after germination while penetrating the stigma tissues to reach an elongation of 0.3-0.4 mm/hours all along the style, and then doubled their speed of elongation when entering the ovary area (Fig. S1b, Table S2).

Fertilisation and embryo development

In both floral morphs, each locule of the pentacarpellate ovary has 12 ± 2 ovules (Fig. S2). The anatropous and bitegmic ovules were disposed along a single longitudinal axis on placentae (Figs. 4, 5 and S2). The embryo sac (female gametophyte) was an *Oenothera*-type and composed of only 4 cells: 2 synergids and an egg-cell on the micropyle side, and a single polar

nucleus in the central cell, matching previous observations made on other *Ludwigia* species and other Onagraceae genera (Fig. 4, 5; Rigakishi 1918; Eyde 1977; Tilquin and de Brouwer 1982; Tobe and Raven 1986).

In L-morph flowers, 24 hours after pollination, 98% of self-pollen tubes stopped their elongations, lately, in between the ovarian area and the beginning of the first integuments (Fig. 4.a, b). In these figures, the pollen tubes seem to be located before the nucellus-epistase out of the embryo sac and did not succeed to pass the synergids. However, it is always difficult to obtain sections showing all together, the synergids, egg cell and central cell which compromise the possibility to identify precisely where the pollen tube stopped. The embryo sacs found with self-pollen tubes stopped didn't develop and degenerated three days after pollination (Fig. 4.c). In the greenhouse, self-pollinated L-morph flowers abscised three days after pollination which is consistent with the temporality of our histological observations (Fig. 4a). In comparison, the abscission of the unpollinated flowers of L-morphs occurred four days after emasculation, when protected with a cellophane bag. Under aniline blue fluorescence, we observed that 2% of self-pollen tubes (6/300) in L-morph flowers succeeded to reach the embryo sac and that only one self-fecundation event was observed over the 300 self-pollinated L-morph studied ovules from the ovary sections (Fig. 4b).

In S-morph, regardless of pollen origin, and in L-morph when inter-morph cross-pollinated, the first cell divisions of the embryos began two to three days after pollination (Fig. 5). From five days after pollination, the nucellus gradually began to disintegrate while the embryo continued to develop and grow. At 15 days, the nucellus disappeared completely, giving way to exalbuminous embryo development, which concluded with a viable seed 45 days after pollination.

Fruit production in self-incompatible L-morph

In the greenhouse, during summer, only four very “small fruits” containing one, four, five and nine seeds respectively developed over 1600 studied L-morph flowers that were hand-pollinated with self-pollen only (Fig. 6). Considering that 60 ovules on average were initially available per flower, the rate of self-fertilisation was 0.02% (i.e., 19 seeds from 1600 x 60=96000 potential ovules available). In the greenhouse, during the fall, at the end of the flowering season, 25 very “small fruits” containing between one and ten seeds for a total of 98 seeds (Fig. 6), gave a rate of self-fertilisation of 0.1% (98 on 96000 potential ovules), thus 5-fold more than obtained in July, during the high fruiting period. All 30 S-morph flowers, which were self-pollinated as a control, developed into 30 fruits containing a total of 1800 seeds, with a constant number of 60 seeds per fruit both in July and September (Fig. 6).

To validate the results obtained in experimental conditions, we then assessed the production of "small fruits" in five L-morph and five S-morph *in situ* populations (Table S1). We found between 15 and 35 “small fruits” per m^2 in self-incompatible monomorphic L-morph populations. All the “small fruits” collected *in situ* contained one to 15 seeds per fruit, as we obtained in experimental conditions in greenhouse. We counted a production of 92 to 217 seeds per m^2. In the five self-compatible S-morph populations, we counted 384 to 864 fruits per m^2. On five of these fruits per population, we counted 50 to 70 seeds per fruit, giving an estimation of 19200 to 51840 seeds per m^2 (Table S1). All seeds from “small fruits” obtained in greenhouse and *in-situ* germinated, and developed into viable seedlings (Table S1).

Discussion

Our results showed that European invasive populations of *Lgh* reproduced using a mixed mating system, whatever the floral morph, both in a common garden and in natural populations.

Pollen grains and stigma surfaces of both floral morphs showed similar sizes and shapes. In the self-incompatible L-morph flowers, self-pollen tubes were only stopped when reaching the ovaries, before penetrating the ovules. These observations argue for a prezygotic, ovarian, late acting self-incompatibility system in L-morph flowers of *Lgh*, literally corresponding to Gibbs classification (2014). As commonly observed in this kind of SI system (Seavey and Bawa 1986; Gibbs 2014b), a small proportion of self-pollen (0.02%), increasing by a factor of 5 at the end of the flowering seasons, succeeded to fertilize the ovules and to develop into seeds. All the resulting seeds obtained then developed into viable seedlings. In the self-compatible S-morph, all self-pollens succeeded in fertilizing the embryo-sacs and successfully developed into viable seeds then seedlings. Yet, in the two *Lgh* floral morphs, inter-morph pollen tubes always elongated faster than self-pollen tubes, which may give advantage to intermorph crosses when inter-morph pollen is available.

The prezygotic LSI system in *Lgh*: a rare but already observed SI system

In European invasive populations, *Lgh* is a heterostylous species with two floral morphologies, a long-styled prezygotic late-acting self-incompatible L-morph and a short-styled self-compatible S-morph. Most heterostylous species with SI systems also often present differences in size and shape of pollen and stigmas papillae (Dulberger et al. 1975; Dulberger 1992; Barrett and Shore 2008) which was not the case of *Lgh*. Less frequently, as we observed in *Lgh* populations, heterostylous SI species show similar pollen shape and papillae structure between floral morphs, as previously observed in *Turnera joelii* and *Turnera scabra* (Turneraceae, Safavian and Shore 2010) and in the heterostylous LSI species *Narcissus tazetta* L. (Dulberger, 1964), *Narcissus triandrus* L. (Sage et al. 1999), and *Narcissus papyraceus* (Barrett and Shore 2008; Simon-Porcar et al. 2015). In these last three Amaryllidaceae species, self-pollen tubes also stopped lately and prezygotically, as we observed in *Lgh*. Such LSI system is not specific

to heterostylous species as it was also observed in homomorphic species like in *Ipomopsis aggregate* from the Polemoniaceae (Sage et al. 2006).

In the order of Myrtales, 76 of 674 species of the Onagraceae family were reported to be self-incompatible (Raven 1979). Two of these species, *Oenothera organensis* and *Oenothera rhombipetala*, were formally demonstrated to be self-incompatible by studying their pollen tube progression after self and cross pollinations and reported to involve a homomorphic GSI system (Emerson 1939; Bali and Hecht 1965). In *Epilobium obcordatum*, another self-incompatible species of the Onagraceae family, most of the self-pollen tubes stopped before entering the embryo sac (Seavey and Carter 1996) and suspected to mate using an ovarian, LSI system (Seavey and Bawa 1986). However, contrary to our observations in *Lgh*, the rare self-fertilised ovules of *E. obcordatum* present substantial rates of post-zygotic failures (Seavey and Carter 1996).

Overall, LSI have been previously reported in two other families of the Myrtales order: in the Myrtaceae family, in *Acca sellowiana* (Finatto et al. 2011), in *Melaleuca alternifolia* (Baskorowati et al. 2010) and in *Eucalyptus globulus* (Pound et al. 2002), and in six Vochysia species of the Vochysiaceae family (Oliveira and Gibbs 1994). Together with our results, these observations question a possible wider occurrence of LSI in the Myrtales order. Our results may add a third family of the Myrtales order as developing an LSI system.

Permeability of LSI L-morph flowers: a delayed selfed mating system?

Our results showed that, despite the LSI developed in the L-morph flowers, self-fertilisation still occurred at a low, stable rate in both experimental and *in situ* populations. This type of mating system enabling for some self-fertilisation especially at the end of flowering season, named delayed selfing, has been reported in multiple angiosperm species as a recurrent mating

strategy (Lloyd 1992; Sakai 1995; Goodwillie and Weber 2018). In such species, self-pollination is blocked or delayed until the opportunity for outcrossing has passed. Delayed selfing is thought to have evolved in preferentially allogamous species because it would provide some reproductive assurance when populations suffer from the lack of compatible pollen (Goodwillie and Weber 2018; Ruane et al. 2020; Xu 2021).

A preferential allogamy mating system even in the self-compatible S-morph?

Before our study, we expected that individuals of the self-compatible S-morph preferentially mates using selfing (Kerbs et al. 2020). Surprisingly, the elongation dynamics of pollen tubes highlighted another process susceptible to favour allogamy in *Lgh*, even in the self-compatible S-morph. Inter-morph pollen tubes elongated significantly faster than self-pollen tubes while progressing along the style. This phenomenon has already been described in several species with a LSI mating system, like in *Camellia oleifera* and in *Crotalaria juncea* (Liao et al. 2014; Rangappa Thimmaiah et al. 2018). But faster elongation of inter-morph pollen tubes does not occur in all LSI species. For example, self- and cross-pollen tubes present similar elongation speed in *Aconitum kusnezofii* or *Cyrtanthus breviflorus* (Vaughton et al. 2010; Hao et al. 2012). Further studies should determine whether the advantage of inter-morph pollen tube elongation also applies when flowers are pollinated with a mixture of self and inter-morph pollens in controlled pollinations, as reported in *Campsis radicans* (Bertin et al. 1989) or using paternity analysis on seeds produced after free pollination in *in situ* populations that mix the two floral morphs, as reported in *Luculia pinceana* (Zhou et al. 2015).

Consequences of LSI for invasive populations of *Lgh*

Our results showed that invasive populations only composed of the self-incompatible L-morph still produced few small fruits containing few seeds resulting from self-fertilization, in similar proportions to what we obtained in experimental conditions. If these self-fertilized seeds remained limited in number at the scale of an individual, we estimated from our measures in quadrats that populations in Loire watershed still produced from 92 to 217 seeds per m^2 which can all potentially germinate and resulted into viable seedlings. Delayed selfing in the L-morph *Lgh* populations resulted in a consequential quantity of viable floating seeds that may contribute to their local regeneration, seed bank and dissemination. In the invasion context, individuals capable of self-fertilization or uniparental reproduction can regenerate a new population in the absence of compatible partners (Baker 1955; Barrett et al. 2008). Accordingly, a recent survey on 1,752 angiosperm species showed that selfing ability fosters directly and indirectly alien plant establishment (Razanajatovo et al. 2016). In contrast, 75% of the worldwide *Lgh* invasive populations are monomorphic L-morph self-incompatible populations (Portillo-Lemus et al. 2021) which may constitute an anomaly to 'Baker's Law' (Baker 1955). But, we highlighted here that the L-morph certainly mated using a LSI system but also used delayed selfing in European invasive populations, better fitting Baker hypotheses. This mixed mating system with preferential allogamy and delayed selfing, never described before this study, must be considered for the future management plan of *Lgh* invasive populations.

Beyond a system with a compatible morph and a self-incompatible morph, that may have suggested simple mating systems, our study revealed a more complex picture with a mixed mating system combining preferential allogamy and delayed selfing in a different way in the two floral morphs. Our results encouraged to explore in more details fertilization in plants to better characterise their mating system and their consequences for populations.

Acknowledgements

This research was supported by FEDER funds from Région Centre-Val de Loire and by Agence de l'eau Loire-Bretagne (grant Nature 2045, programme 9025 (AP 2015 9025)). FEDER also financed the doctoral grant of L. Portillo and the technical assistance salary of M. Harang. The authors thank Diane Corbin (FRAPNA Loire - Ecopôle du Forez), and Guillaume Le Roux (Réserve Naturelle Val d'Allier Châtel-de-Neuvre) for making plant material available. We thank the Experimental Unit of Aquatic Ecology and Ecotoxicology (U3E) 1036, Institut national de recherche pour l'agriculture, l'alimentation et l'environnement (INRAE, which is part of the research infrastructure Analysis and Experimentations on Ecosystems-France, for help with the maintenance of plants.

Data availability

Here lien Zenodo

Author Contribution

LP and DB designed this project. MH, MB, LP and DB performed all experiments. JH participated in capsule husking. LP, SS and DB analysed data and wrote the manuscript. All authors approved the manuscript.

References

Baker HG (1955) Self-compatibility and establishment after'long-distance'dispersal. Evolution 9:347–349

Bali PN, Hecht A (1965) The genetics of self-incompatibility in Oenothera rhombipetala. Genetica 36:159–171. https://doi.org/10.1007/BF01557151

Barlow BA, Forrester J (1984) Variation in Indumentum Morphology in the Melaleuca leucadendra Complex (Myrtaceae). Brunonia 7:277–288. https://doi.org/10.1071/bru9840277

Barranco D, Arroyo J, Santos-Gally R (2019). Avoiding sexual interference: herkogamy and dichogamy in style dimorphic flowers of Narcissus broussonetii (Amaryllidaceae), AoB PLANTS, 11(4): plz038, https://doi.org/10.1093/aobpla/plz038

Barrett SC, Colautti RI, Eckert CG (2008) Plant reproductive systems and evolution during biological invasion. Molecular ecology 17:373–383

Barrett SC, Cole WW, Herrera CM (2004) Mating patterns and genetic diversity in the wild daffodil Narcissus longispathus (Amaryllidaceae). Heredity 92:459–465

Barrett SCH (2019) 'A most complex marriage arrangement': recent advances on heterostyly and unresolved questions. New Phytologist 224:1051–1067. https://doi.org/10.1111/nph.16026

Barrett SCH, Cruzan M (1994a) Variation in incompatibility in heterostylous plants. In: Genetic control of self-incompatibility and reproductive development in flowering plants, Springer. Dordrecht, pp 189–219

Barrett SCH, Cruzan MB (1994b) Incompatibility in heterostylous plants. In: Williams EG, Clarke AE, Knox RB (eds) Genetic control of self-incompatibility and reproductive development in flowering plants. Springer Netherlands, Dordrecht, pp 189–219

Barrett SCH, Shore JS (2008) New Insights on Heterostyly: Comparative Biology, Ecology and Genetics. In: Self-Incompatibility in Flowering Plants. Springer Berlin Heidelberg, Berlin, Heidelberg, pp 3–32

Baskorowati L, Moncur MW, Cunningham SA, et al (2010) Reproductive biology of Melaleuca alternifolia (Myrtaceae) 2. Incompatibility and pollen transfer in relation to the breeding system. Aust J Bot 58:384–391. https://doi.org/10.1071/BT10036

Beardsell DV, Knox RB, Williams EG (1993) Breeding System and Reproductive Success of Thryptomene calycina (Myrtaceae). Aust J Bot 41:333–353. https://doi.org/10.1071/bt9930333

Bertin RI, Barnes C, Guttman SI (1989) Self-Sterility and Cryptic Self-Fertility in Campsis radicans (Bignoniaceae). Botanical Gazette 150:397–403. https://doi.org/10.1086/337785

Busch JW, Schoen DJ (2008) The evolution of self-incompatibility when mates are limiting. Trends in Plant Science 13:128–136. https://doi.org/10.1016/j.tplants.2008.01.002

Charlesworth D, Vekemans X, Castric V, Glémin S (2005) Plant self-incompatibility systems: a molecular evolutionary perspective: Research review. New Phytologist 168:61–69. https://doi.org/10.1111/j.1469-8137.2005.01443.x

Chen X, Hao S, Wang L, et al (2012) Late-acting self-incompatibility in tea plant (Camellia sinensis). Biologia 67:347–351. https://doi.org/10.2478/s11756-012-0018-9

Cheptou P-O (2012) Clarifying Baker's law. Annals of botany 109:633–641

Cohen JI (2010) "A case to which no parallel exists": The influence of Darwin's Different Forms of Flowers. American Journal of Botany 97:701–716. https://doi.org/10.3732/ajb.0900395

Dandelot S (2004) Les *Ludwigia* spp. invasives du Sud de la France : historique, biosystématique, biologie et écologie. Université d'Aix-Marseille

Darwin C (1877) The different forms of flowers on plants of the same species. D. Appleton

de Nettancourt D (1997) Incompatibility in angiosperms. Sex Plant Reprod 10:185–199. https://doi.org/10.1007/s004970050087

Dickinson HG, Crabbe MJC, Gaude T (1992) Sporophytic Self-Incompatibility Systems: S Gene Products. International Review of Cytology 140:525–561. https://doi.org/10.1016/S0074-7696(08)61108-0

Dulberger R (1992) Floral Polymorphisms and Their Functional Significance in the Heterostylous Syndrome. In: Barrett SCH (ed) Evolution and Function of Heterostyly. Springer, Berlin, Heidelberg, pp 41–84

Dulberger R, Heslop-Harrison J, Lewis D (1975) Intermorph structural differences between stigmatic papillae and pollen grains in relation to incompatibility in Plumbaginaceae. Proceedings of the Royal Society of London Series B Biological Sciences 188:257–274. https://doi.org/10.1098/rspb.1975.0018

Duminil J, Fineschi S, Hampe A, et al (2007) Can population genetic structure be predicted from life-history traits? The American Naturalist 169:662–672

Dutartre MA, CEMAGREF F, Secretariat E, Brunel MS (2011) PEST RISK ANALYSIS FOR: Ludwigia grandiflora. EPPO

Ellegren H, Galtier N (2016) Determinants of genetic diversity. Nat Rev Genet 17:422–433. https://doi.org/10.1038/nrg.2016.58

Emerson S (1939) A Preliminary Survey of the Oenothera Organensis Population. Genetics 24:524–537

Eyde RH (1977) Reproductive structures and evolution in Ludwigia (Onagraceae). I. Androecium, placentation, merism. Annals of the Missouri Botanical Garden 644–655

Ferrer MM, Good SV (2012) Self-sterility in flowering plants: preventing self-fertilization increases family diversification rates. Annals of Botany 110:535–553. https://doi.org/10.1093/aob/mcs124

Finatto T, Dos Santos KL, Steiner N, et al (2011) Late-acting self-incompatibility in Acca sellowiana (Myrtaceae) 1. Australian journal of botany 59:53–60

Fujii S, Kubo K, Takayama S (2016) Non-self- and self-recognition models in plant self-incompatibility. Nature Plants 2:16130. https://doi.org/10.1038/nplants.2016.130

Gibbs PE (2014a) Late-acting self-incompatibility - the pariah breeding system in flowering plants. New Phytologist 203:717–734. https://doi.org/10.1111/nph.12874

Gibbs PE (2014b) Late-acting self-incompatibility – the pariah breeding system in flowering plants. New Phytologist 203:717–734. https://doi.org/10.1111/nph.12874

Gibbs PE, Bianchi M (1993) Post-pollination Events in Species of Chorisia (Bombacaceae) and Tabebuia (Bignoniaceae) with Late-acting Self-incompatibility. Botanica Acta 106:64–71. https://doi.org/10.1111/j.1438-8677.1993.tb00339.x

Gibbs PE, Bryan GW (1986) Reproductive Failure in Populations of the Dog-Whelk, Nucella Lapillus, Caused by Imposex Induced by Tributyltin from Antifouling Paints. Journal of the Marine Biological Association of the United Kingdom 66:767–777. https://doi.org/10.1017/S0025315400048414

Goodwillie C, Weber JJ (2018) The best of both worlds? A review of delayed selfing in flowering plants. American Journal of Botany 105:641–655

Grossenbacher DL, Brandvain Y, Auld JR, et al (2017) Self-compatibility is over-represented on islands. New Phytol 215:469–478. https://doi.org/10.1111/nph.14534

Hao Y-Q, Zhao X-F, She D-Y, et al (2012) The Role of Late-Acting Self-Incompatibility and Early-Acting Inbreeding Depression in Governing Female Fertility in Monkshood, Aconitum kusnezoffii. PLOS ONE 7:e47034. https://doi.org/10.1371/journal.pone.0047034

Hieda S, Kaneko Y, Nakagawa M, Noma N (2020) Ludwigia grandiflora (Michx.) Greuter & Burdet subsp. hexapetala (Hook. & Arn.) GL Nesom & Kartesz, an invasive aquatic plant in Lake Biwa, the largest lake in Japan. Acta Phytotaxonomica et Geobotanica 71:65–71

Hinata K, Watanabe M, Toriyama K, Isogai A (1993) A Review of Recent Studies on Homomorphic Self-Incompatibility. International Review of Cytology 143:257–296. https://doi.org/10.1016/S0074-7696(08)61877-X

Igic B, Bohs L, Kohn JR (2004) Historical inferences from the self-incompatibility locus. New Phytologist 161:97–105. https://doi.org/10.1046/j.1469-8137.2003.00952.x

Igic B, Lande R, Kohn JR (2008) Loss of Self-Incompatibility and Its Evolutionary Consequences. International Journal of Plant Sciences 169:93–104. https://doi.org/10.1086/523362

Kao TH, McCubbin AG (1996) How flowering plants discriminate between self and non-self pollen to prevent inbreeding. PNAS 93:12059–12065

Kerbs B, Crawford DJ, White G, et al (2020) How rapidly do self-compatible populations evolve selfing? Mating system estimation within recently evolved self-compatible

populations of Azorean Tolpis succulenta (Asteraceae). Ecology and Evolution 10:13990–13999. https://doi.org/10.1002/ece3.6992

Liao T, Yuan D-Y, Zou F, et al (2014) Self-sterility in Camellia oleifera may be due to the prezygotic late-acting self-incompatibility. PLoS One 9:e99639

Lloyd DG (1992) Self- and Cross-Fertilization in Plants. II. The Selection of Self-Fertilization. International Journal of Plant Sciences 153:370–380. https://doi.org/10.1086/297041

Medrano M, Requerey R, Karron JD, Herrera CM (2012) Herkogamy and mate diversity in the wild daffodil Narcissus longispathus: beyond the selfing–outcrossing paradigm in the evolution of mixed mating. Plant Biology 14:801–810

Nesom GL, Kartesz JT (2000) Observations on the Ludwigia uruguayensis Complex (Onagraceae) in the United States. Castanea 65:123–125

Oliveira P, Gibbs P (1994) Pollination biology and breeding systems of six Vochysia species (Vochysiaceae) in Central Brazil. Journal of Tropical Ecology 509–522

Portillo-Lemus LO, Bozec M, Harang M, et al (2021) Self-incompatibility limits sexual reproduction rather than environmental conditions in an invasive water primrose. Plant-Environment Interactions 2:74–86. https://doi.org/10.1002/pei3.10042

Pound LM, Wallwork MAB, Potts BM, Sedgley M (2002) Self-incompatibility in Eucalyptus globulus ssp. globulus (Myrtaceae). Australian Journal of Botany 50:365–372

Rangappa Thimmaiah M, Choudhary SB, Sharma HK, et al (2018) Late-acting self-incompatibility: a barrier to self-fertilization in sunnhemp (Crotalaria juncea L.). Euphytica 214:19. https://doi.org/10.1007/s10681-017-2096-9

Raven PH (1979) A survey of reproductive biology in Onagraceae. New Zealand Journal of Botany 17:575–593. https://doi.org/10.1080/0028825X.1979.10432572

Razanajatovo M, Maurel N, Dawson W, et al (2016) Plants capable of selfing are more likely to become naturalized. Nature communications 7:1–9

Rigakishi MI (1918) Studies on the Embryo Sac and Fertilization in Oenothera. Annals of Botany 279–318

Ruane LG, Mangum SM, Horner KM, Moeller DA (2020) The opportunity for outcrossing varies across the geographic range of the primarily selfing Clarkia xantiana ssp. parviflora. American Journal of Botany 107:1198–1207. https://doi.org/10.1002/ajb2.1510

Ruaux B (2008) Les plantes envahissantes des corridors fluviaux: traits biologiques, impacts de *Ludwigia peploides* et *L. grandiflora* en Loire moyenne et implications pour la gestion. Université François Rabelais

Safavian D, Shore JS (2010) Structure of styles and pollen tubes of distylous Turnera joelii and T. scabra (Turneraceae): are there different mechanisms of incompatibility between the morphs? Sexual plant reproduction 23:225–237

Sage TL, Bertin RI, Williams EG (1994) Ovarian and other late-acting self-incompatibility systems. In: Williams EG, Clarke AE, Knox RB (eds) Genetic control of self-incompatibility and reproductive development in flowering plants. Springer Netherlands, Dordrecht, pp 116–140

Sage TL, Price MV, Waser NM (2006) Self-sterility in Ipomopsis aggregata (Polemoniaceae) is due to prezygotic ovule degeneration. American Journal of Botany 93:254–262. https://doi.org/10.3732/ajb.93.2.254

Sage TL, Strumas F, Cole WW, Barrett SCH (1999) Differential ovule development following self- and cross-pollination: the basis of self-sterility in Narcissus triandrus (Amaryllidaceae). American Journal of Botany 86:855–870. https://doi.org/10.2307/2656706

Sakai S (1995) Evolutionarily Stable Selfing Rates of Hermaphroditic Plants in Competing and Delayed Selfing Modes with Allocation to Attractive Structures. Evolution 49:557–564. https://doi.org/10.1111/j.1558-5646.1995.tb02287.x

Santos-Gally R, Gonzalez-Voyer A, Arroyo J (2013) Deconstructing Heterostyly: The Evolutionary Role of Incompatibility System, Pollinators, and Floral Architecture. Evolution 67:2072–2082. https://doi.org/10.1111/evo.12087

Seavey SR, Bawa KS (1986) Late-acting self-incompatibility in angiosperms. Bot Rev 52:195–219. https://doi.org/10.1007/BF02861001

Seavey SR, Carter SK (1996) Ovule fates in Epilobium obcordatum (Onagraceae). American Journal of Botany 83:316–325. https://doi.org/10.1002/j.1537-2197.1996.tb12712.x

Simon-Porcar VI, de Castro A, Herrero M, Arroyo J (2015) Ovarian self-incompatibility in Narcissus papyraceus (Amaryllidaceae) is the result of a pre-zygotic response. Botanical Journal of the Linnean Society 177:629–643

Takayama S, Isogai A (2005) SELF-INCOMPATIBILITY IN PLANTS. Annu Rev Plant Biol 56:467–489. https://doi.org/10.1146/annurev.arplant.56.032604.144249

Thouvenot L, Haury J, Thiebaut G (2013) A success story: water primroses, aquatic plant pests. Aquatic Conservation: Marine and Freshwater Ecosystems 23:790–803

Tilquin JP, de Brouwer K (1982) Aspects cytologiques de la reproduction sexuée dans le genre Fuchsia. Bulletin de la Société Royale de Botanique de Belgique/Bulletin van de Koninklijke Belgische Botanische Vereniging 33–42

Tobe H, Raven PH (1986) A comparative study of the embryology of Ludwigia (Onagraceae): characteristics, variation, and relationships. Annals of the Missouri Botanical Garden 768–787

Vaughton G, Ramsey M, Johnson SD (2010) Pollination and late-acting self-incompatibility in Cyrtanthus breviflorus (Amaryllidaceae): implications for seed production. Annals of Botany 106:547–555. https://doi.org/10.1093/aob/mcq149

Xu K (2021) The coevolution of flower longevity and self-fertilization in hermaphroditic plants. Evolution n/a: https://doi.org/10.1111/evo.14303

Zhou W, Barrett SCH, Wang H, Li D-Z (2015) Reciprocal herkogamy promotes disassortative mating in a distylous species with intramorph compatibility. New Phytologist 206:1503–1512. https://doi.org/10.1111/nph.13326

Figures and Support information

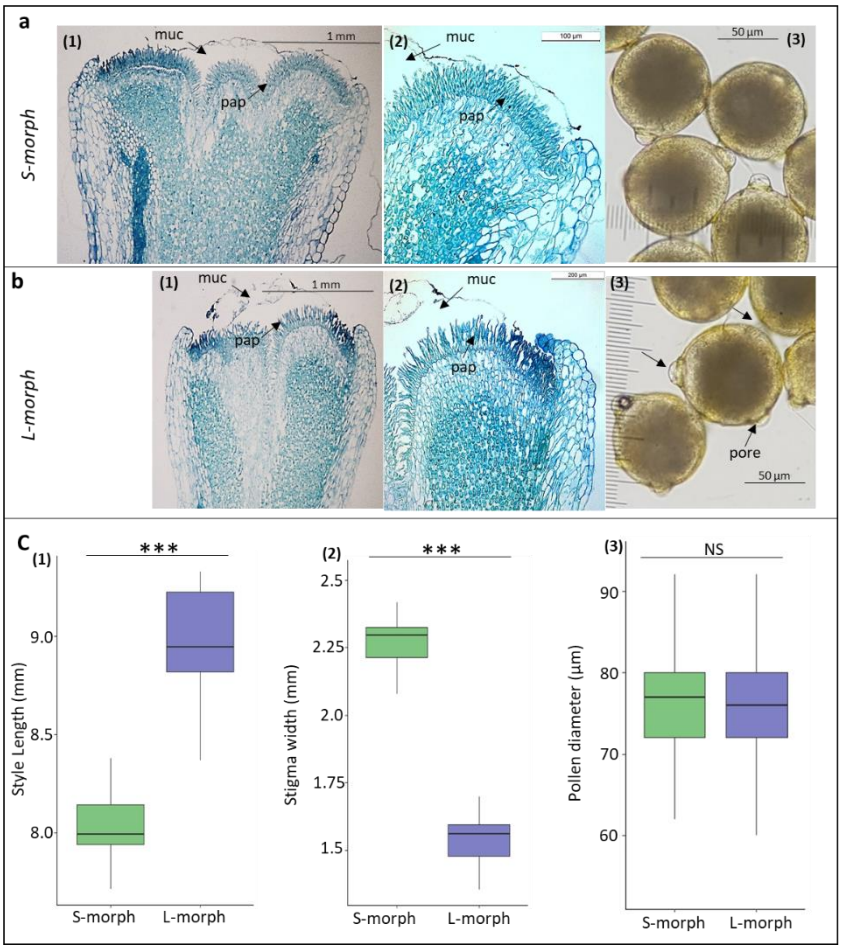

Figure 1: Stigma and pollen morphologies in both floral morphs of *Ludwigia grandiflora* subsp. *hexapetala*.

- Stigma section of S-morph (a 1, 2) and L-morph (b 1, 2) under the 10x (a1, b1) and 20x (a2, b1) objectives of optic microscope stained with toluidine blue O. Stigma sections of the stigma have a thickness of 15 µm. In both floral morphs, the stigma was filled with mucilage (mu) (a1-2, b1-2,). Both floral morphs showed the same shape of stigmatic papillae (pap).

- Pollen morphologies of S-morph (a3) and L-morph (b3) under 20X objective of optical microscope. Both morphotypes shared the same shape and size of pollen (a3, b3) and the same diameter of pollen (c3).

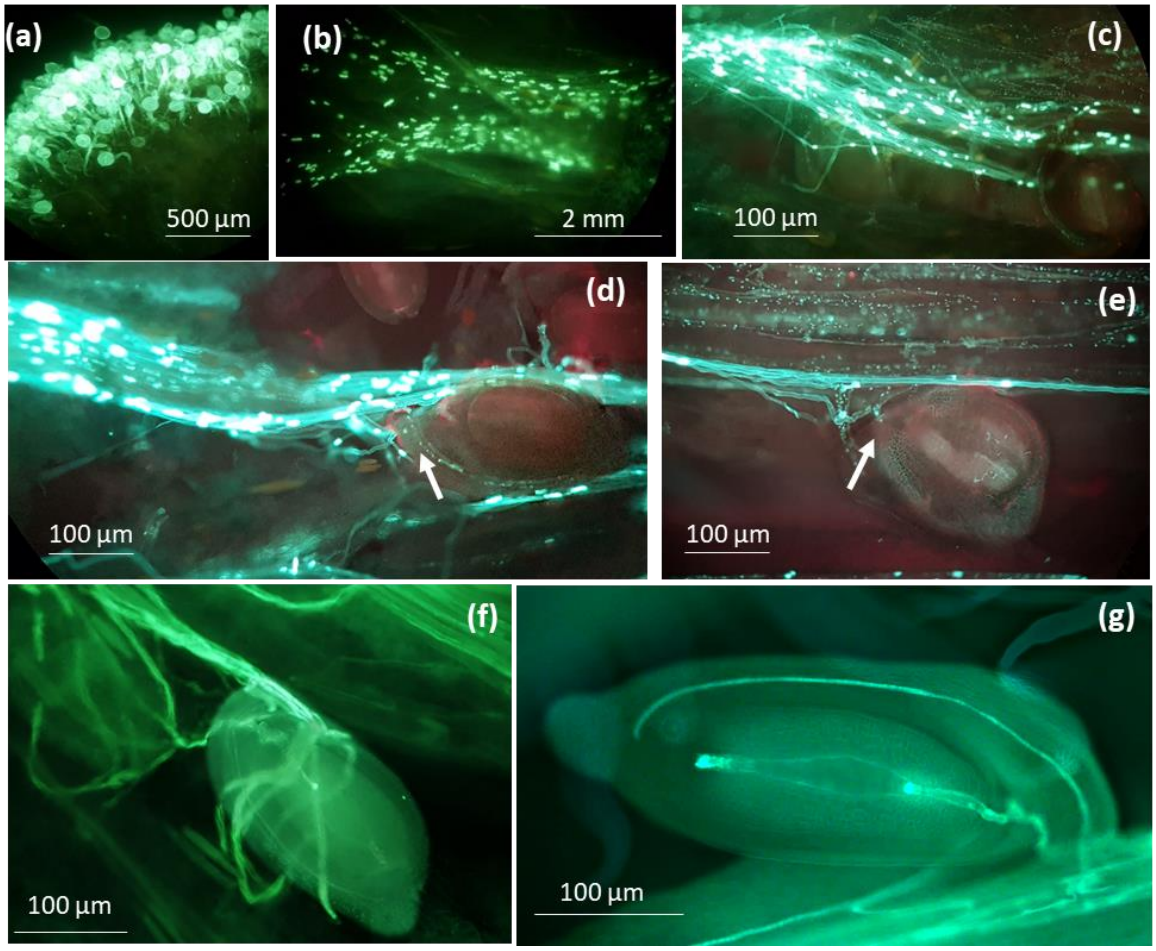

Figure 2: Fluorescence aniline blue staining of self-pollen tube in L-morph pistils (a-f).

a) Pollen grains germination on a stigma surface (zoom 10X); b) Pollen tubes elongating in a style (zoom 2.5X); c, d, e) Pollen tubes in the ovarian area (zoom 20X); f) Pollen tubes in the area of embryo sac (noticed for 6 pollen tubes over 300 studied). g) Pollen tubes in the area of embryo sac in S-morph ovary after self-pollination.

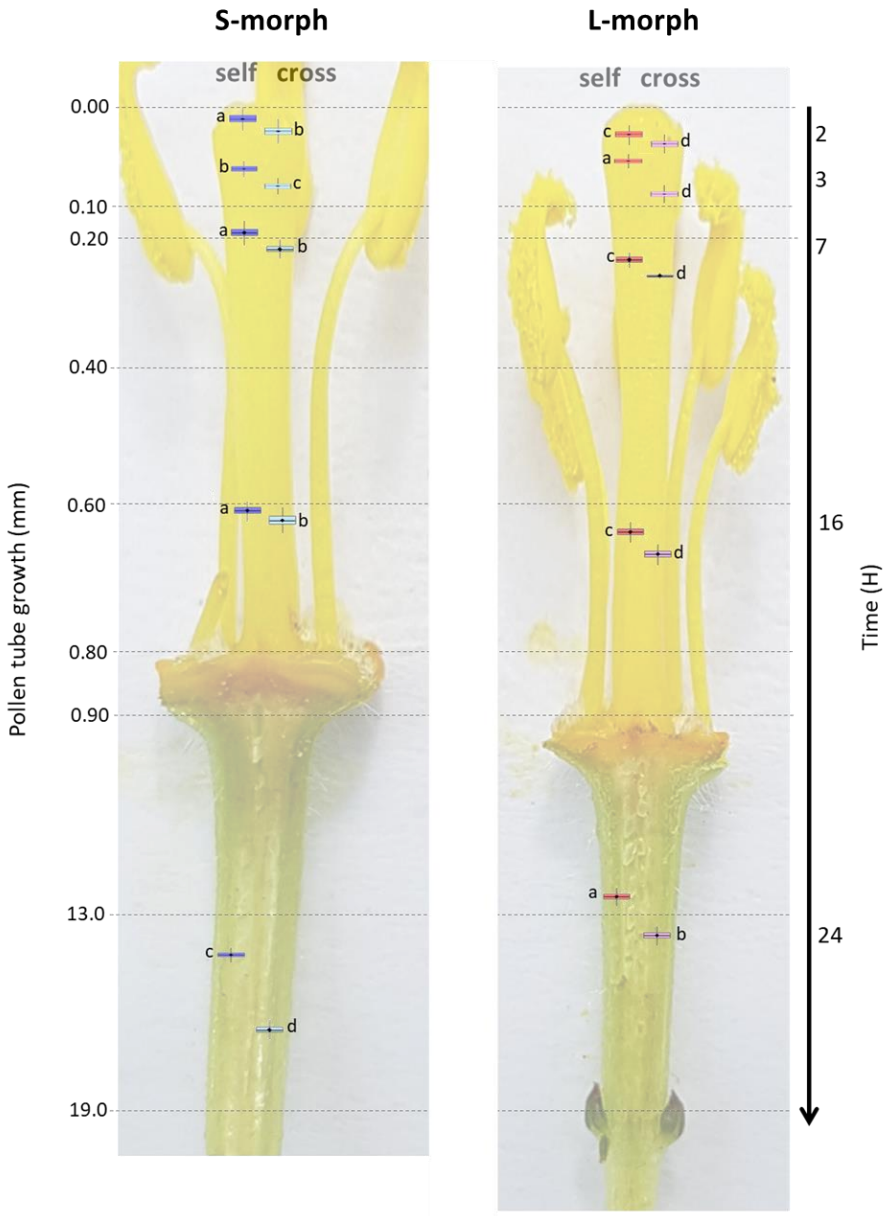

Figure 3: Kinetic of pollen tube elongations in both floral morphs in *Ludwigia grandiflora* subsp. *hexapetala*.

a) Kinetic of pollen tube elongations in S-morph styles when self- and cross-pollinated (left, blue and sky-blue boxes respectively); b) Kinetic of pollen tube elongations in L-morph style when self- and cross-pollinated (right, red and pink boxes respectively). Significance letters were obtained using a Tukey's honestly significant difference (HSD) post-hoc comparisons of the means. In both floral morphs, cross-pollen tubes elongated faster than self-pollen.

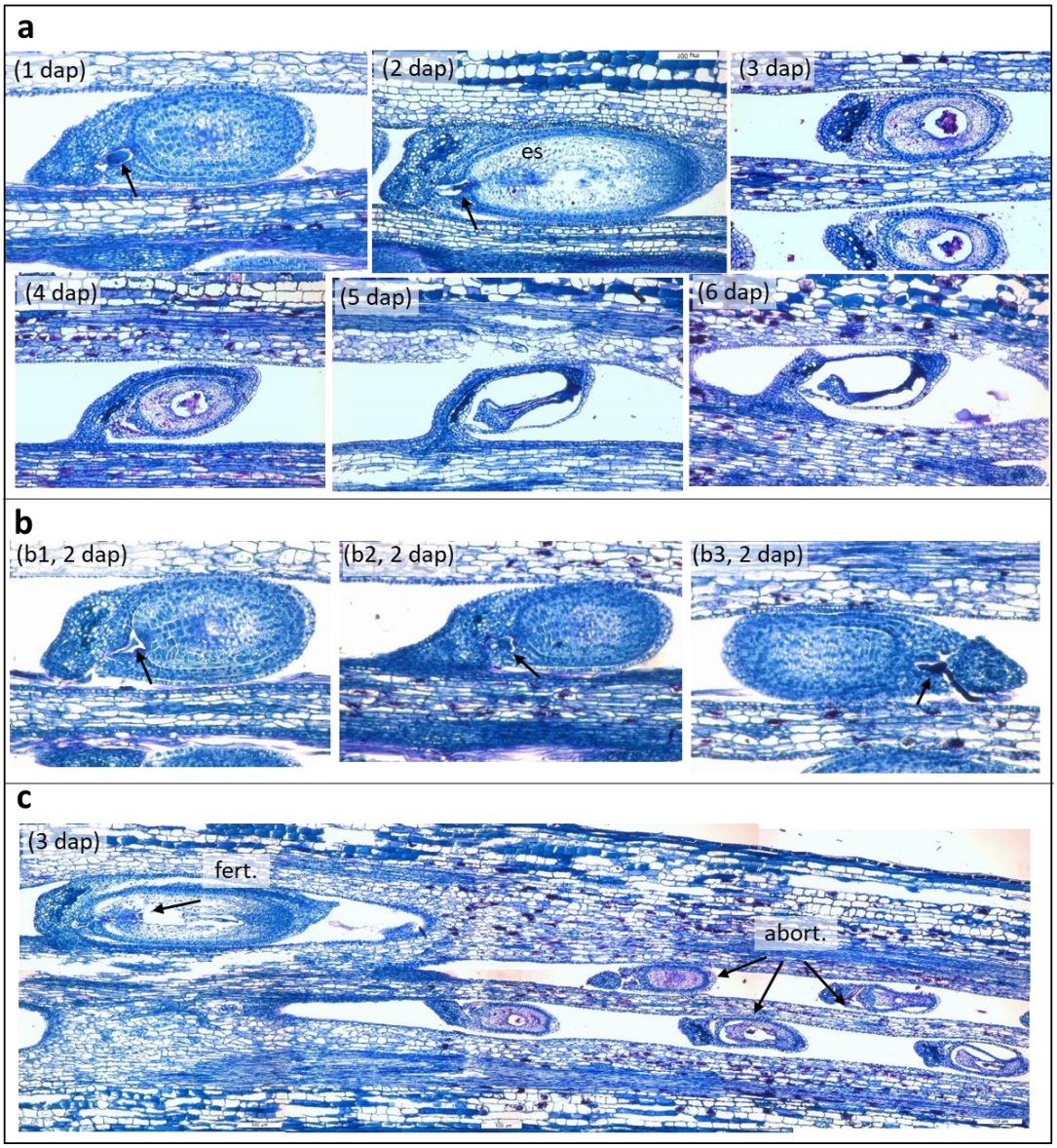

Figure 4: Temporal evolution of embryo sacs, ovules and ovaries in self-incompatible L-morph flowers after self-pollination.

a) Abortive ovules sections after 1, 2, 3, 5 and 6 days after self-pollination (dap); b) Self-pollen tubes that stopped their elongations two days after self-pollination (dap) in three different ovules (1 to 3). The arrows indicate the tips of the self-pollen tube stopped between the ovarian tissues and the beginning of the first cell layers of the ovule integuments (see figure 5a for a comprehensive representation of the ovule parts); c) Example of a rare self-fertilisation event (fert.) obtained three days after self-pollination (dap) informing the “small fruit” formation.

Only ~0.33% ovules were fertilised (1/300 ovules observations) (fertilisation = fert; abortive ovules= abort). All sections stained with toluidine blue O (zoom 10X). See figure 5 a comprehensive representation of the ovule parts.

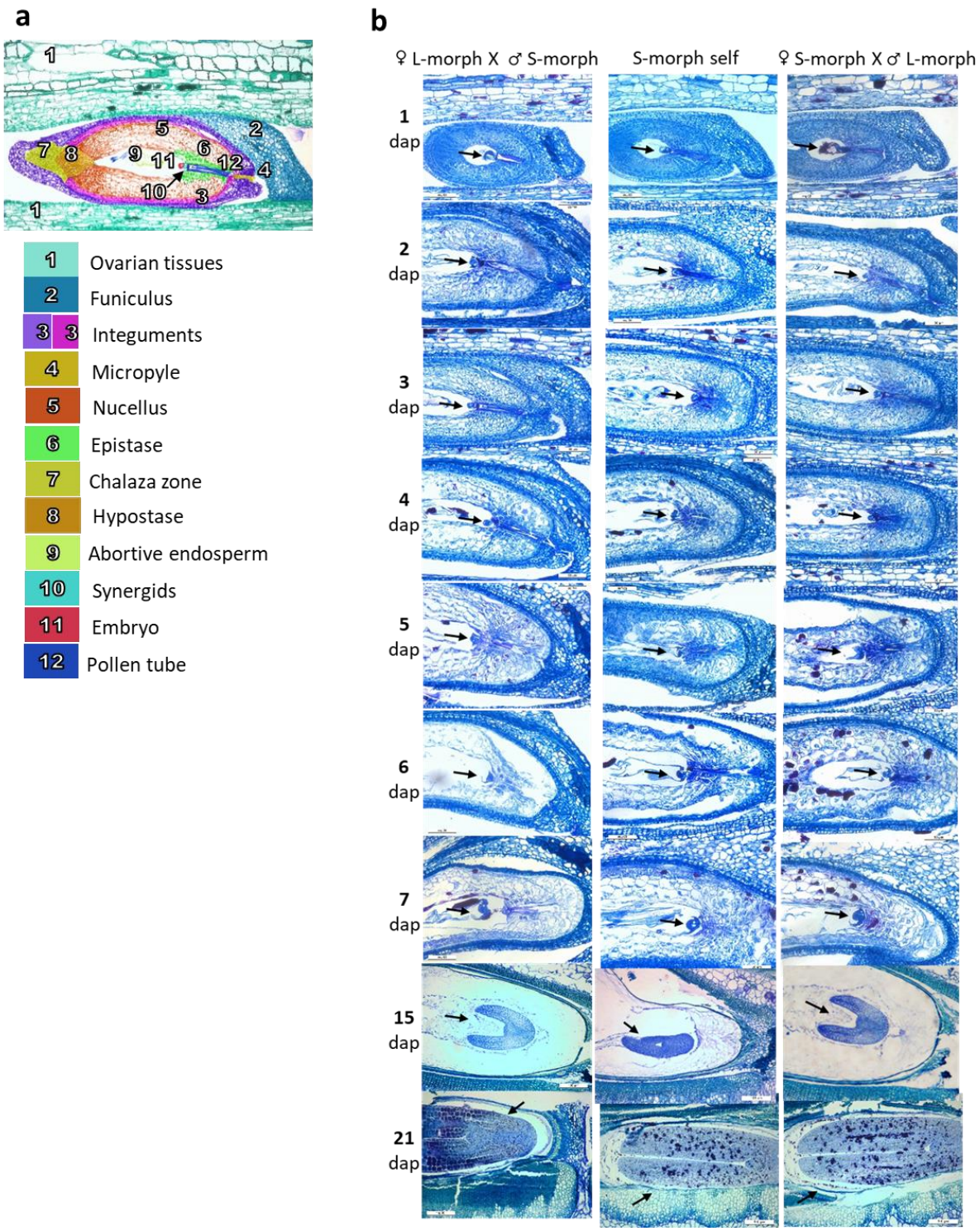

Figure 5: Fertilisation and embryonic development after cross and self-pollinating the self-incompatible L-morph and the self-compatible S-morph flowers.

a - A comprehensive, colorized scheme of the different tissue parts of a L-morph ovule 3 days after disassortative pollination.

b- Evolution of the ovules 1, 2, 3, 4, 5, 6, 7, 15, and 21 days after pollen deposition on the stigmas (dap): (1) L-morph ovules after cross-pollination (♀ L-m X ♂ S-m); (2) S-morph ovules after self-pollination; (3) S-morph ovules after cross-pollination (♀ S-m X ♂ L-m).

The arrows indicate the development of embryo. All sections were stained with toluidine blue O, 20X zoom under optical microscope.

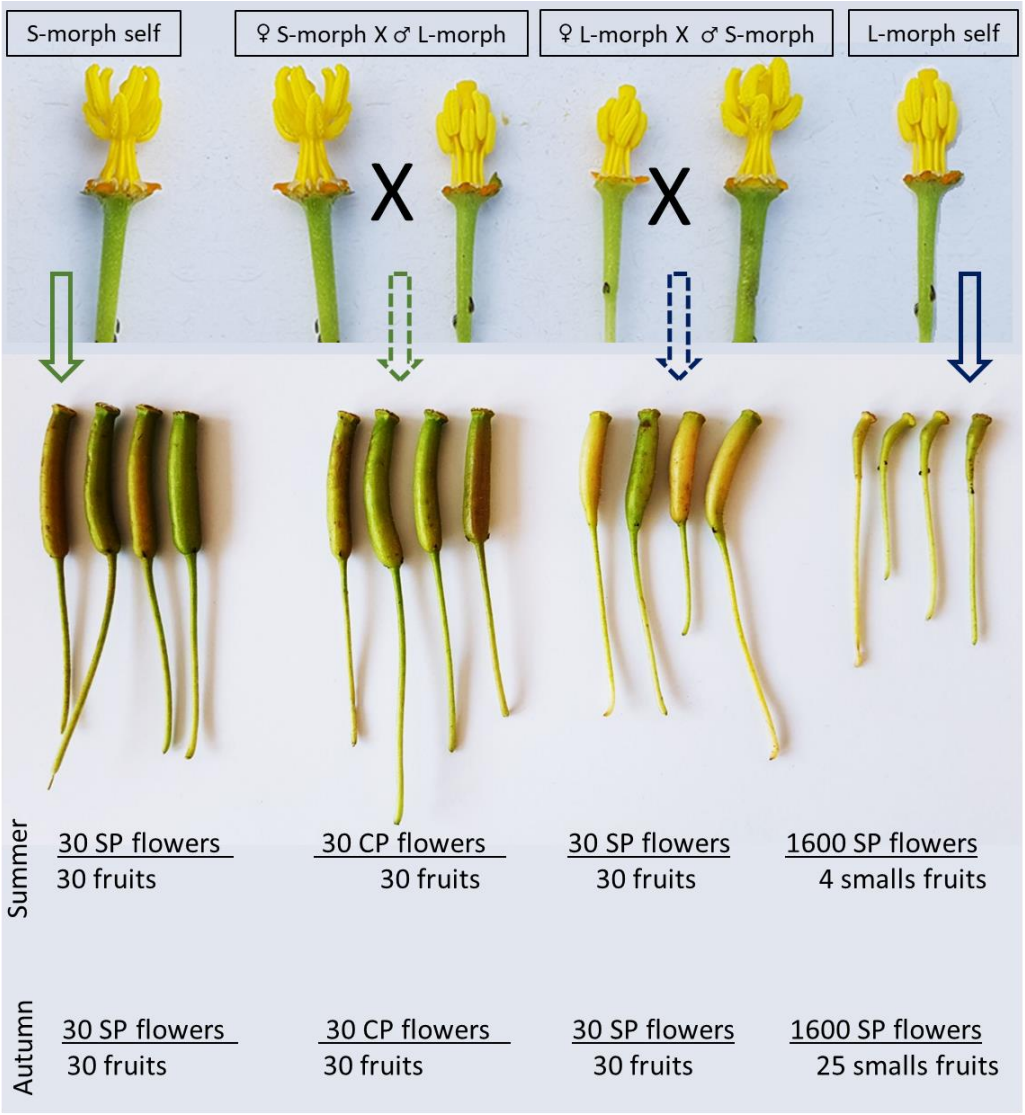

Figure 6: Summary of the fruit-set obtained from S-morph and L-morph flowers after hand-controlled pollination (SP = Self-pollination; CP = Cross-pollination) in summer and autumn.

- All S-morph flowers produced fully-seeded fruits, in summer and autumn, both after self- and cross-pollinations.

- All L-morph flowers produced fully-seeded fruits, in summer and autumn, when pollinated with S-morph pollen (L-morph x S-morph).

- 0.25% and 1.56% of L-morph flowers produced “small fruits” in summer and autumn when self-pollinated. These “small fruits” contained one to nine seeds that all successfully germinated and grew into viable seedlings.

Table S1: Fruit-set, seed-set and germination rate in S-morph and L-morph *in situ* populations.

Fruit-set, seed-set and mean number of seeds produced in the studied *in situ* monomorphic populations of *Lgh*. Seed-set productions per m^2 in monomorphic S-morph populations were estimated by counting the number of seeds produced by fruits in 5 quadrats of $1m^2$ and multiplied by the mean number of counted fruits per quadrat. Seed-set productions per quadrat in L-morph populations are reported as the exhaustive number of seeds within all the fruits found in the quadrat.

Population	GPS Location		Fruitfulness & Floral morph	average number of seeds per fruit	Fruitset per m^2	Seedset per m^2	germination percentage
Chambéon	45°41'03.4"N	4°12'12.1"E	Fruitless L-morph	4.18	22	92	95.67%
Châtel-de-Neuvre	46°24'05.4"N	3°19'10.1"E	Fruitless L-morph	6.40	15	96	93.75%
Gilly-sur-Loire	46°31'40.6"N	3°48'25.7"E	Fruitless L-morph	6.79	28	190	93.68%
Pouilly-sur-Loire	47°16'48.4"N	2°57'25.2"E	Fruitless L-morph	5.68	19	108	89.81%
Orléans	47°53'41.3"N	1°55'48.6"E	Fruitless L-morph	6.20	35	217	94.47%
Pont-de-Cé	47°25'40.7"N	0°31'28.9" W	Fruitful S-morph	55	792	43560	90.30%
Mazerolles	47°23'17.3"N	1°28'07.4" W	Fruitful S-morph	60	864	51840	96.71%
Saint-Aignan-sur-Cher	47°16'19.8"N	1°22'32.1"E	Fruitful S-morph	55	528	29040	89.46%
Lac-de-Maine	47°27'34.7"N	0°35'30.8" W	Fruitful S-morph	50	624	31200	98.12%
Sabot-d'Or	47°19'14.1"N	2°15'24.4" W	Fruitful S-morphe	50	384	19200	91.55%

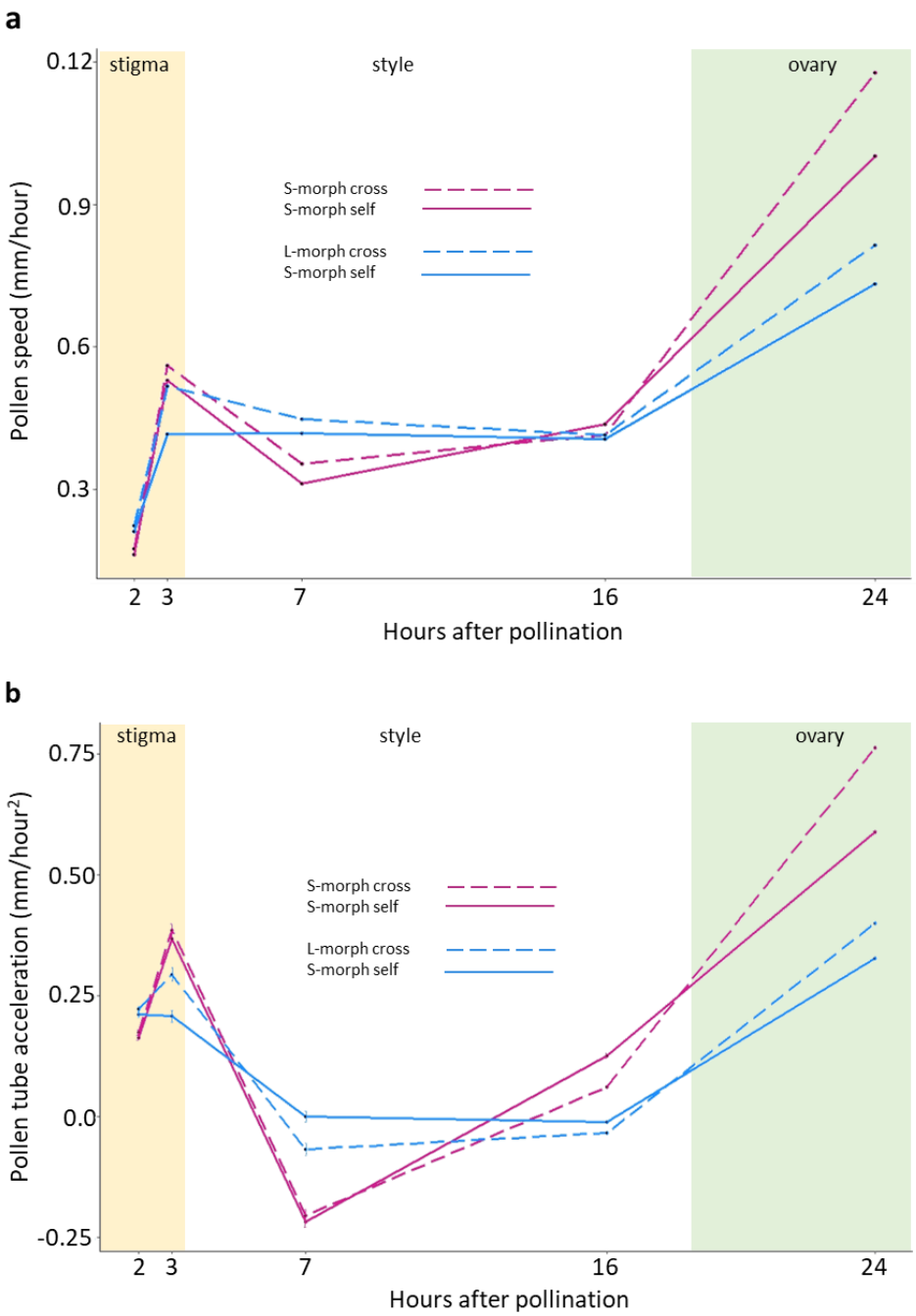

Figure S1: Speed and acceleration of pollen tube elongations in both floral morphs in *Ludwigia grandiflora* subsp. *hexapetala* after self- and cross-pollinated.

Red = S-morph, blue = L-morph; solid line = self-pollination (self) and dotted line=cross-pollination (cross). a) Speed of pollen tube elongations in both S-morph and L-morph styles after self and cross pollinations. b) Acceleration of pollen tube elongations in both S-morph and L-morph styles after self and cross pollinations.

Table S2: Analyses of the variations of pollen tube elongation along time (a), speed (b) and acceleration of pollen tube elongation (b) in both floral morphs in *Ludwigia grandiflora* subsp. *hexapetala* after self- and cross-pollinations.

(a)

```
Analysis of Variance Table
Response: Growth of pollen tubes =>  anova(lm(Length ~ Pollination_condition * Hours_after_pollinations))
```

Anova Table (Type III tests)

	Df	Sum_Sq	Mean_Sq	F_value	Pr(>F)
Pollination_conditions	3	1.94571	0.64857	6094	< 2.2e-16 ***
Residuals	796	0.08472	0.00011		
Pollination_conditions	3	1.89545	0.63182	4700.7	< 2.2e-16 ***
Residuals	796	0.10699	0.00013		
Pollination_conditions	3	46.067	15.3558	80721	< 2.2e-16 ***
Residuals	796	0.151	0.0002		
Pollination_conditions	3	26.1592	8.7197	65513	< 2.2e-16 ***
Residuals	796	0.1059	0.0001		
Pollination_conditions	3	1315.28	438.43	3306413	< 2.2e-16 ***
Residuals	796	0.11	0		

Significance codes: .001 “***”; .01 “**”; .05 “*”; non significant “NS.”

Analysis of Variance Table
Tukey test; alpha = 0.05
Response: length of pollen tubes

Pollination_conditions	HAP	mean	SD	groups of signif
S-morph_self	2	0.3251328	0.0102478	a
S-morph x L-morph	2	0.349352	0.0099562	b
L-morph_self	2	0.4207731	0.0103041	c
L-morph x S-morph	2	0.4449497	0.0106426	d
S-morph_self	3	0.8550793	0.0103665	b
S-morph x L-morph	3	0.909661	0.0124761	c
L-morph_self	3	0.8374607	0.0101908	a
L-morph x S-morph	3	0.9615144	0.0129607	d
S-morph_self	7	2.1001969	0.0163765	a
S-morph x L-morph	7	2.3251743	0.0136882	b
L-morph_self	7	2.5056041	0.0113881	c
L-morph x S-morph	7	2.7542894	0.0131105	d
S-morph_self	16	6.0289593	0.0117017	a
S-morph x L-morph	16	6.0539117	0.0136438	b
L-morph_self	16	6.1577877	0.0098296	c
L-morph x S-morph	16	6.4826446	0.0104896	d
S-morph_self	24	14.0489390	0.0099906	c
S-morph x L-morph	24	15.4732020	0.0099158	d
L-morph_self	24	12.01793	0.0130931	a
L-morph x S-morph	24	12.9937810	0.0125769	b

Signif. codes: a -> b -> c -> d = p-value <2.2e-16

(b)

```
Analysis of Variance Table
Response: speed of pollen tubes =>  anova(lm(speed ~ Pollination_condition))
```

Anova Table (Type III tests)

	Df	Sum_Sq	Mean_Sq	F_value	Pr(>F)
Pollination_conditions	3	0.48643	0.162142	6094	< 2.2e-16 ***
Residuals	796	0.02118	0.000027		
Pollination_conditions	3	2.26998	0.75666	5629.5	< 2.2e-16 ***
Residuals	796	0.10699	0.00013		
Pollination_conditions	3	2.30357	0.76786	64582	< 2.2e-16 ***
Residuals	796	0.00946	0.00001		
Pollination_conditions	3	0.104195	0.034732	21137	< 2.2e-16 ***
Residuals	796	0.001308	0.000002		
Pollination_conditions	3	23.7891	7.9297	3827337	< 2.2e-16 ***
Residuals	796	0.0016	0		

Significance codes: .001 “***”; .01 “**”; .05 “*”; non significant “NS.”

Analysis of Variance Table
Tukey test; alpha = 0.05
Response: Speed of pollen tubes

Pollination_conditions	HAP	mean	SD	groups of signif
morph-S_self	2	0.1625664	0.0051239	d
morph-S x morph-L	2	0.174676	0.0049781	c
morph-L_self	2	0.2103866	0.005152	b
morph-L x morph-S	2	0.2224748	0.0053213	a
morph-S_self	3	0.5298404	0.0103665	b
morph-S x morph-L	3	0.559422	0.0124761	a
morph-L_self	3	0.4176024	0.0101908	d
morph-L x morph-S	3	0.5166561	0.0129607	c
morph-S_self	7	0.3109203	0.0040941	d
morph-S x morph-L	7	0.3534147	0.0034221	c
morph-L_self	7	0.417389	0.002847	b
morph-L x morph-S	7	0.4483104	0.0032776	a
morph-S_self	16	0.4366003	0.0013002	a
morph-S x morph-L	16	0.4143728	0.001516	b
morph-L_self	16	0.4057916	0.0010922	c
morph-L x morph-S	16	0.4143976	0.0011655	b
morph-S_self	24	1.0024951	0.0012488	b
morph-S x morph-L	24	1.177403	0.0012395	a
morph-L_self	24	0.7325065	0.0016366	d
morph-L x morph-S	24	0.8138629	0.0015721	c

Signif. codes: a -> b -> c -> d = P value <2.2e-16

(c)

```
Analysis of Variance Table
Response: accelleration of pollen tubes =>  anova(lm(acceleration~
Pollination_condition ))
```

Anova Table (Type III tests)

	Df	Sum_Sq	Mean_Sq	F_value	Pr(>F)
Pollination_conditions	3	1.94571	0.64857	6094	< 2.2e-16 ***
Residuals	796	0.08472	0.00011		
Pollination_conditions	3	1.89545	0.63182	4700.7	< 2.2e-16 ***
Residuals	796	0.10699	0.00013		
Pollination_conditions	3	46.067	15.3558	80721	< 2.2e-16 ***
Residuals	796	0.151	0.0002		
Pollination_conditions	3	26.1592	8.7197	65513	< 2.2e-16 ***
Residuals	796	0.1059	0.0001		
Pollination_conditions	3	1315.28	438.43	3306413	< 2.2e-16 ***
Residuals	796	0.11	0		

Significance codes: .001 “***”; .01 “**”; .05 “*”; non significant “NS.”

Analysis of Variance Table
Tukey test; alpha = 0.05
Response: acceleration of pollen tubes

Pollination_conditions	HAP	mean	SD	groups of signif
morph-S_self	2	0.1625664	0.0051239	d
morph-S x morph-L	2	0.174676	0.0049781	c
morph-L_self	2	0.2103866	0.005152	b
morph-L x morph-S	2	0.2224748	0.0053213	a
morph-S_self	3	0.3672739	0.0112325	b
morph-S x morph-L	3	0.384746	0.0129094	a
morph-L_self	3	0.2072158	0.0116108	d
morph-L x morph-S	3	0.2941812	0.0137249	c
morph-S_self	7	-0.21892	0.0107856	d
morph-S x morph-L	7	-0.206007	0.0131338	c
morph-L_self	7	-0.000213	0.0106224	a
morph-L x morph-S	7	-0.068346	0.0132985	b
morph-S_self	16	0.12568	0.0044317	a
morph-S x morph-L	16	0.0609581	0.0038266	b
morph-L_self	16	-0.011597	0.0029275	c
morph-L x morph-S	16	-0.033913	0.0034387	d
morph-S_self	24	0.5880975	0.0016601	b
morph-S x morph-L	24	0.7630302	0.0019039	a
morph-L_self	24	0.3267149	0.0018812	d
morph-L x morph-S	24	0.3994653	0.0019593	c

Signif. codes: a -> b -> c -> d = P value <2.2e-16

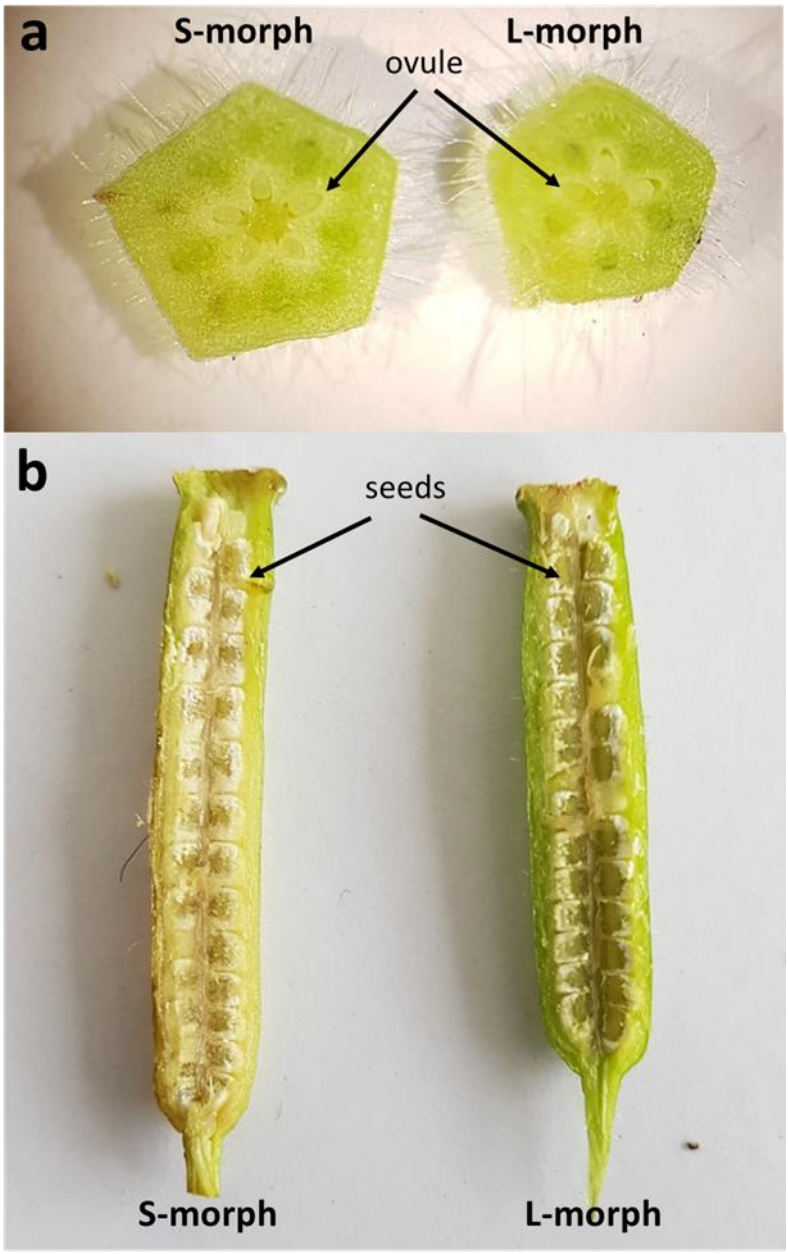

Figure S2: a) transversal and b) longitudinal sections of petaloculate ovary from 5-merous floral morphs of *Ludwigia grandiflora* subsp. *hexapetala*.